Journal of Engineering Sciences
Vol 11, Issue 4 ,April/2020
ISSN NO:0377-9254

# LOW TEMPERATURE PHOTOLUMINESCENCE STUDY OF CdS NANOCRYSTALS

Nilesh Pote[1]
[1] Department of Physics, K. J. Somaiya College, Kopargaon, Maharashtra, India
[*]Corresponding author e mail:nilesh.pote2008@gmail.com

***Abstract*—CdS nanocrystals with size 2.3 nm are synthesized by colloidal synthesis. Their structural, optical and electrical characterization is studied. The synthesized nanocrystals are highly crystalline verified by XRD analysis. By photoluminescence measurements photoluminescence quantum yield of nanocrystals found to be around 10%. From low temperature PLE measurements four energy levels were attributed to transitions of energy levels $1S_{3/2} \rightarrow 1S$, $1P_{3/2} \rightarrow 1P$, $1S_{1/2} \rightarrow 1S$ and $1P_{1/2} \rightarrow 1P$. The energy level transitions $1S_{3/2} \rightarrow 1S$, $1P_{3/2} \rightarrow 1P$, $1S_{1/2} \rightarrow 1S$ and $1P_{1/2} \rightarrow 1P$ blue shifts with decreasing temperature.***

***Keywords*— Nanocrystals, CdS Nanocrystals, Energy levels, Low temperature photoluminescence.**

## 1. INTRODUCTION

In semiconductor NCs, quantum confinement effects observed when one or more dimensions of the NCs approaches the size of bulk Bohr exciton radius ($a_B$) given by equation [1]:

$$a_B = \frac{4\pi\epsilon_\infty \hbar^2}{m_0 e^2}\left(\frac{1}{m_e^*}+\frac{1}{m_h^*}\right) \quad \text{-----(1)}$$

Here, $\varepsilon_\infty$ is the high frequency relative dielectric constant of the medium, $m_e^*$and $m_h^*$are effective masses of the electron and hole, respectively (both in units of $m_0$), and $m_0$ is rest mass of the electron. For CdS NCs exciton Bohr radius is 2.92nm. Quantum confinement effect can be understood by considering a relationship between free and confined particles [2],[3]. For a free particle in a periodic potential the energy and the crystal momentum 'ħk' may both be precisely defined, while the position is not. When the radius of a particle approaches the size of the Bohr exciton radius, electrons and hole is confined. Thus in case of confined particles (localized) the uncertainty in position decreases, so that momentum is no longer well defined. The wider range of momentum translates to a higher average energy. As a result the electron of a confined particle has higher energy compared to that in a bulk solid. Due to the spatial confinement of the charge carriers, the valence and conduction bands split into discrete, quantized, electronic energy levels. The spacing of the electronic energy levels and the band gap increases with decreasing particle size. This is because the electron hole pairs are now much closer together and the Coulomb interaction between them can no longer be neglected giving overall higher kinetic energy. The increase in band gap can be observed experimentally by the blue-shift in the absorption spectrum. Sometimes, even visually one can observe change in colour of sample with size of NCs. Theoretical models, such as the effective mass approximation (EMA) [4],[5] empirical tight-binding method (ETBM)[6],[7] effective bond orbital model (EBOM)[8] and empirical pseudo-potential method (EPM)[9],[10],[11] have been proposed to explain quantum size effects.

The simplest model to explain quantum size effects is EMA. As a first approximation the masses of the electron and hole are taken to be the effective masses of electron and hole in the bulk semiconductor. According to EMA, the quantum-size effects can be described by a "particle in a box" model, in which the electron motion is restricted in all three dimensions by impenetrable walls [12],[13],[14]. An exciton (electron-hole pair) created by absorption of photon is considered as particle in a rigid sphere of radius R. This model was first developed by Efros *et al.* [12] using an infinite potential well and excluding coulomb interaction. Brus *et al.* [14] included the coulomb interactions and in addition considered the effect of the matrix's dielectric constant on exciton binding energies. In EMA, the valence band and the conduction band are taken to be parabolic at their extrema, i.e. near k = 0. The E-k curves are parabolic (of the form $E = \hbar^2k^2/2m$). But as k increases, the shape of the E-k curve becomes complex and depends on the direction of electron transport with respect to the principal crystal directions. Away from k = 0, E-k curve, can still be

described by a parabolic relation $E = \hbar^2k^2/2m^*$ where m is replaced by m*. Here m* is the effective mass of the electron given by,

$$m^* = \frac{\hbar^2}{\frac{\partial^2 E}{\partial k^2}} \quad \text{-----(2)}$$

Eigen value of the lowest excited state is given by [14],

$$E(R) = E_g + \frac{\hbar^2}{2}\left(\frac{1}{m_e^*} + \frac{1}{m_h^*}\right)\frac{\pi^2}{R^2} - 1.786\frac{e^2}{\epsilon R} - 0.248E_{Ry}^* \quad \text{-----(3)}$$

Where, R is the cluster radius and $E_{Ry}^*$ is the effective Rydberg energy given by,

$$E_{Ry}^* = \frac{e^4}{2\varepsilon^2\hbar^2\left(\frac{1}{m_e}+\frac{1}{m_h}\right)} \quad \text{-----(4)}$$

The first term in eigenvalue equation, represents the band gap of the bulk semiconductor. The second term represents a particle in a box type eigenvalue and has $1/R^2$ dependence, which is the increase in the kinetic energy due to the localization of the exciton in the rigid sphere. The third term is the Coulomb energy term with 1/R dependence. It comes into picture because the electron and hole interact via Coulomb attraction. The last term is a result of the spatial correlation effect and gives a measure of the correlation between electron and hole. Equation 5 represents the last term in which energy is inversely proportional to square of the permittivity of material hence become significant for semiconductors with small dielectric constant and this term is independent of size of a NCs. In the early time, Ekimov *et al.* [10] reported the absorption spectra of CdS NCs ranging in size from 30 to 800 Å. The optical absorption spectra of NCs have revealed that exciton energies are blue shifted compared to the value in bulk materials, and it can be understood in terms of quantum confinement of the exciton. Wang *et al.* [11] have experimentally investigated the dependence of the lowest exciton energy of CdS NCs on the cluster size.

In the present work CdS NCs with sizes 4.6 nm were synthesized with oleic acid capping. The phase of nanocrystals verified by X ray diffraction spectroscopy. The synthesized nanocrystals were highly crystalline. Size and energy gap of nanocrystals calculated by absorption spectroscopy. Quantum efficiency measurements performed using photoluminescence excitation spectroscopy which shows that CdS nanocrystals have size dependent optical properties. To study low temperature evolution of energy levels photoluminescence excitation measurements were performed. Six energy levels peaks observed and attributed to excited states.

## 2.EXPERIMENTAL SECTION

**2.1 CHEMICALS:** Cadmium oxide (99.99%), sulfur powder (99.98%) were purchased from Aldrich. Oleic acid (OA, tech. 90%), 1-octadecene (ODE, tech. 90%) (ACS, 98.0101.0%). All organic solvents were purchased from EM Sciences. All chemicals were used directly without any further purification unless otherwise stated

**2.2 SYNTHESIS PROCEDURE:** Synthesis of CdS NCs performed by reported method with slight modification [15]. Briefly a mixture of CdO (0.0256 g, 0.2 mmol), oleic acid (0.3 mL), and octadecene [ODE (6 g)] was heated to 260 $^0$C in a three-neck round-bottom reaction flask under argon. When the solution turned clear, 1 mL of sulfur solution (0.1 mol/l) in ODE was swiftly injected into this hot solution, and the reaction mixture was allowed to cool down to 240 $^0$C for 5 minutes. The reaction was stopped and cooled down to 50 $^0$C when the CdS core reached a desired size. An in situ purification procedure was performed as described below. An excess of methanol (~10 mL), an extraction solvent, was added to the flask with stirring at 50 $^0$C. When ODE layer and methanol layer were separated, the upper methanol layer was taken by syringe to remove un-reacted precursors and side products. The purification procedure was repeated three times. Purified CdS NCs with size 4.6 nm were used for characterizations. Phase of NCs was determined by using x-ray diffraction (XRD) employing Bruker D8 advance powder x-ray diffractometer, with Cu $K_\alpha$ ($\lambda$ = 1.5402 Å) as an incident radiation. Linear optical absorption studies were performed using Perkin Elmer Lambda 950 spectrophotometer to estimate the gap between the highest occupied molecular orbital (HOMO) and the lowest unoccupied molecular orbital (LUMO). Photoluminescence measurements were carried out with Jobin-Yvon PL spectrometer.

## 3.RESULTS AND DISCUSSION

All In order to obtain CdS NCs, oleic acid (OA) which acts as a capping ligand concentration is taken to 0.3 mL keeping all other reaction parameters same during synthesis. It is observed that the amount of OA determines the size of CdS NCs. After synthesis of CdS NCs X ray diffraction (XRD) pattern recorded to confirm formation of

CdS NCs. Fig.1 depicts XRD pattern for different size CdS NCs. The *d* values are closely matching with standard ICDD PDF data (sheet no.80 – 0019) of that of cubic zinc blende CdS. The phase has not changed even when sizes of NCs are varied.

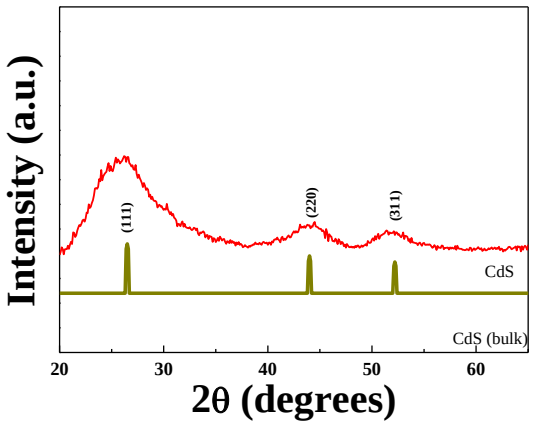


Fig.1 XRD of CdS nanocrystals having sizes CdS (2.3nm) radius.

Lattice parameter for CdS (radius 2.3nm) calculated by XRD were NCs 5.722A$^0$. The Lattice parameters of all nanocrystals is in close agreement with bulk CdS, represented in table 1. The lattice constant values also depicted in table 1 for CdS1 nanocrystals were in close agreement with ICDD PDF data.

**Table1. Comparasion of d values and lattice constants obtained with XRD spectra and ICDD PDF data.**

| **Sample** | **$d_{111}$(A$^0$)** | **$d_{220}$(A$^0$)** | **$d_{311}$(A$^0$)** | **Lattice const. a(A$^0$)** |
|---|---|---|---|---|
| CdS | 3.41 | 1.99 | 1.7 | 5.72 |
| Bulk CdS(Cubic) | 3.36 | 2.06 | 1.7 | 5.81 |

Optical absorption measurements are used to estimate NC size with the aid of empirical formula [16],

$$D = (-6.6521 \times 10^{-8})\lambda^3 + (1.9557 \times 10^{-4})\lambda^2 - (9.2352 \times 10^{-2})\lambda + 13.29 \quad \text{----(5)}$$

In the above equations, D (nm) is the size of a given nanocrystal sample, and λ (nm) is the wavelength of the first excitonic absorption peak of the corresponding sample. Using value of λ, which is 399 nm, size of nanocrystals 2.3 nm were estimated and absorption and photoluminescence spectra at room temperature is shown in figure 2. The narrow absorption features of CdS NCs in absorption spectra near bandage indicate focusing of size distribution of the particles in sample.

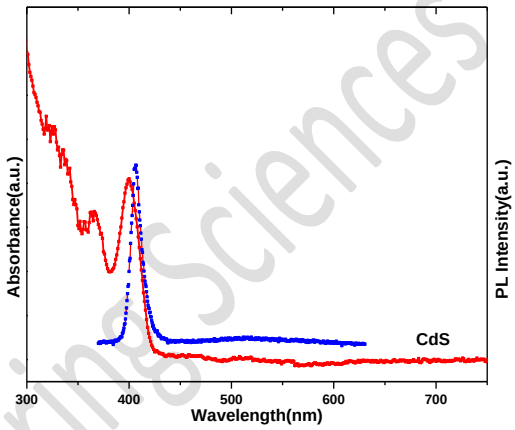


Fig.2 Absorption and photoluminescence spectra of CdS nanocrystals having sizes CdS (2.3nm) radius.

Photoluminescence (PL) emission spectra of CdS nanocrystals depicted in figure 2 recorded at excitation wavelength of 375 nm at room temperature. Photoluminescence efficiency (QE) is also measured found to around 10 %. The PL peaks observed in figure 2 have Gaussian nature with low full width at half maximum which again suggest focusing of particle size. There is also defect level emission observed in all CdS nanocrystals around 560 nm this may be due to surface dangling bonds and surface trap states which also limits quantum efficiency of nanocrystals [17]. Low temperature photolumiscence spectra recorded at room temperature (RT), 250 K, 200 K, 150K, 100K, 50K and 10K shown in figure 3. With decreasing temperature intensity of band edge luminescence enhances with decreasing defect level peak. There is no any shift in peak position was observed at low temperature. FWHM of bandage luminescence also goes on decreasing.

**P**

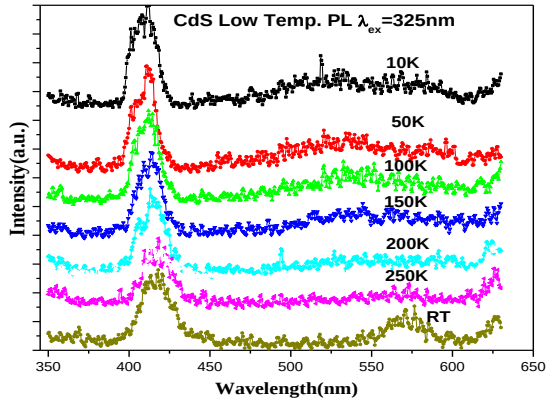


Fig.3 Low temperature photoluminescence spectra of CdS Nanocrystals having sizes CdS (2.3nm) radius.

The photoluminescence excitation (PLE) spectroscopy of CdS NC is shown in Figure 4. The PLE spectra of the nanocrystals exhibit four absorption bands after data fitting and denoted by letters A, B, C, and D at room temperature. Out of six peaks four attributed to energy transitions as A to $1S_{3/2} \rightarrow 1S$, B to $1P_{3/2} \rightarrow 1P$, C to $1S_{1/2} \rightarrow 1S$ and D to $1P_{1/2} \rightarrow 1P$[18, 19, 20]. It was clearly seen from figure 4 that absorption peaks shift to the blue as temperature of the clusters is decreased. This behavior is similar to the size-dependence of the absorption edge and may be illustrated well by quantum-size confinement based on the effective-mass approximation [20].

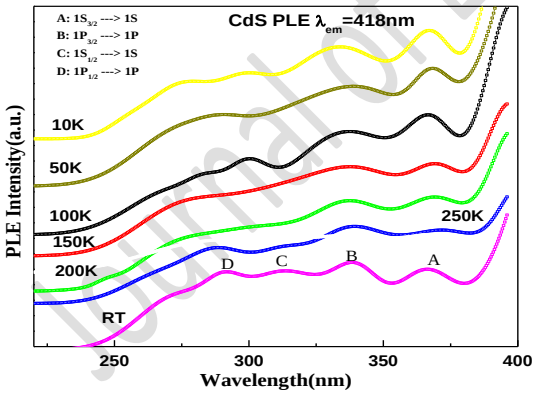


Fig.4 Low temperature photoluminescence excitation spectra of CdS Nanocrystals having sizes CdS (2.3nm) radius.

To understand how these energy levels evolve with size the measurements were repeated several times. The energy level transitions obeserved in CdS as A at 399.67± 0.334nm, B at 368.5 ± 0.334nm, C at 339 ±2nm, D at 324.33 ±1.23nm. as size increses these enerrgy level transitions expected to blue shift [22].

## 4. CONCLUSIONS

CdS nanocrystals with 2.3 nm size were synthesized by colloidal synthesis. Oleic acid which is capping agent during synthesis plays a vital role in determining size of CdS nanocrystals. The synthesized nanocrystals were highly crystalline verified by XRD spectra. The optical absorption spectroscopy was used to find size and HOMO-LUMO gap of NCs. The photoluminescence quantum yield of NCs is around 10%. From low temperature PLE measurements four energy levels were attributed to transitions of energy levels $1S_{3/2} \rightarrow 1S$, $1P_{3/2} \rightarrow 1P$, $1S_{1/2} \rightarrow 1S$ and $1P_{1/2} \rightarrow 1P$. The energy level transitions $1S_{3/2} \rightarrow 1S$, $1P_{3/2} \rightarrow 1P$, $1S_{1/2} \rightarrow 1S$ and $1P_{1/2} \rightarrow 1P$ blue shifts with decreasing temperature.

## REFERENCES

[1] S. V. Gaponenko, Optical Properties of Semiconductor Nanocrystals, 1st ed. Cambridge University Press, 1998, pp. 30-35.

[2] V. I. Klimov, Semiconductor and Metal Nanocrystals, 1st ed. Marcel Dekker New York, 2004, pp. 65-99.

[3] U. Woggon, Optical Properties of Semiconductor Quantum Dots, 1st ed. Springer, 1997, pp. 43-101.

[4] Al. L. Efros and A. L. Efros, "Interband absorption of light in a semiconductor sphere," Soviet Phys. Semicond. vol. 16, pp. 772-775, Jan 1982.

[5] L. E. Brus, "A simple model for the ionization potential, electron affinity, and aqueous redox potentials of small semiconductor crystallites," J. Chem. Phys. Vol. 79, pp. 5566-5571, Dec. 1983.

[6] L. E. Brus, "Electron–electron and electron hole interactions in small semiconductor crystallites: The size dependence of the lowest excited electronic state," J. Chem. Phys. Vol. 80, pp. 4403-4409, May 1984.

[7] S. V. Nair, L. M. Ramaniah, and K. C. Rustagi, "Electron states in a quantum dot in an effective-bond-orbital model," Phys. Rev. B, vol. 45, pp. 5969, Mar. 1992.

[8] N. A. Hill and K. B. Whaley, "Electronic structure of semiconductor nanoclusters: A time dependent theoretical approach," J. Chem. Phys. Vol. 99, pp. 3707-3715, Sep. 1993.

[9] N. A. Hill and K. B. Whaley, "Two-particle calculation of excitonic effects in semiconductor nanocrystals," Chem. Phys. Vol. 210, pp. 117-133, Oct. 1996.

[10] J. P. Conde and A. K. Bhattacharjee, "Exciton states and optical properties of CdSe nanocrystals," Phys. Rev. B, vol. 63, pp. 245318, Jun. 2001.

[11] J. G. Diaz and J. Planelles, "Theoretical characterization of triangular CdS nanocrystals: a tight-binding approach," Langmuir, vol. 20, pp. 11278-11284, Dec. 2004.

[12] G. W. Bryant and W. Jaskolski, "Tight-binding theory of quantum-dot quantum wells: Single-particle effects and near-band-edge structure," Phys. Rev. B, vol. 67, pp. 205320, May 2003.

[13] G. T. Einevoll and Y. C. Chang, "Effective bond-orbital model for acceptor states in semiconductors and quantum dots," Phys. Rev. B, vol. 94, pp. 9683-9697, Nov. 1989.

[14] L. W. Wang and A. Zunger, "Pseudopotential calculations of nanoscale CdSe quantum dots," Phys. Rev. B, vol. 53, pp. 9579, Apr. 1996.

[15] D. Chen, F. Zhao, H. Qi, M. Rutherford, and X. Peng, "Bright and stable purple/blue emitting CdS/ZnS core/shell nanocrystals grown by thermal cycling using a single-source precursor," Chem. Mater. Vol. 22, pp. 1437-1444, Jan. 2010.

[16] W. W. Yu, L. Qu, W. Guo, and X. Peng, "Experimental determination of the extinction coefficient of CdTe, CdSe, and CdS nanocrystals." Chem. Mater. Vol. 15, pp. 2854-2860, July 2003.

[17] M. Tanaka, J. Qi, and Y. Masumoto, "Optical properties of undoped and Mn 2+-doped CdS nanocrystals in polymer," Journal of Crystal Growth, vol. 214, pp. 410-414, June 2000.

[18] J. G. Diaz, J. Planelles, G. W. Bryant, and J. Aizpurua, "Tight-binding method and multiband effective mass theory applied to CdS nanocrystals: Single-particle effects and optical spectra fine structure," J. Phys. Chem. B, vol. 108, pp. 17800-17804, Nov. 2004.

[19] Z. Yu, J. Li, D. B. O'Connor, L. Wang, and P. F. Barbara, "Large resonant stokes shift in CdS nanocrystals," J. Phys. Chem. B, vol. 107, pp. 5670-5674, May 2003.

[20] N. Pote, C. Phadnis, K. Sonawane, V. Sudarsan, S. Mahamunia, "The impact of lattice strain on optical properties of CdS nanocrystals," Solid state communications, vol. 192, pp. 6-9, August 2014.

[21] W. Chen, Y. Xu, Z. Lin, Z. Wang and L. Lin, "Formation, structure and fluorescence of CdS clusters in a mesoporous zeolite," Solid State Communications, vol. 105, pp. 129-134, Jan. 1998.

[22] J. Li, J. B. Xia, "Hole levels and exciton states in CdS nanocrystals," Phys. Rev. B, vol. 62, pp. 12613 – 12616, Nov. 2000.